Open-Shell Character and Second Hyperpolarizabilities of One-Dimensional Chromium(II) Chains: Size Dependence and Bond-Length Alternation Effect

ARTICLE *in* INORGANIC CHEMISTRY · JULY 2014

Impact Factor: 4.76 · DOI: 10.1021/ic501334p · Source: PubMed

Inorganic Chemistry

Article

pubs.acs.org/IC

Open-Shell Character and Second Hyperpolarizabilities of One-Dimensional Chromium(II) Chains: Size Dependence and Bond-Length Alternation Effect

Hitoshi Fukui,[†] Shota Takamuku,[†] Taishi Yamada,[†] Kotaro Fukuda,[†] Taku Takebayashi,[†] Yasuteru Shigeta,[†] Ryohei Kishi,[†] Benoît Champagne,[‡] and Masayoshi Nakano*,[†]

[†]Department of Materials Engineering Science, Graduate School of Engineering Science, Osaka University, Toyonaka, Osaka 560-8531, Japan

[‡]Laboratoire de Chimie Théorique, University of Namur, rue de Bruxelles, 61, B-5000 Namur, Belgium

Supporting Information

ABSTRACT: Using the long-range corrected spin-unrestricted density functional theory (LC-UBLYP) method, we have investigated the longitudinal third-order nonlinear optical (NLO) properties, i.e., the second hyperpolarizabilities γ of open-shell singlet one-dimensional (1D) extended metal atom chain (EMAC) systems, chromium(II) chains Cr^{II}_{2n} (n = 1−4), with different metal−metal bond lengths from the viewpoint of the open-shell character dependences of each d orbital contribution (dσ, dπ, dδ) to γ and of the chain-length dependence of γ. It turns out that the chain length dependences of the open-shell characters of dπ and dδ orbitals at any metal−metal bond length are negligible, while the dσ open-shell character decreases as a function of chain length. The systems display bell-shaped behaviors of γ as a function of the metal−metal bond length, in which the γ values attain maxima for intermediate dσ open-shell character. The maximum γ value (γ_{max}) exhibits remarkable enhancement as a function of chain length. It is also found that the bond length alternation (BLA) significantly affects the γ values and their chain-length dependences. The present results provide the guiding principles for designing transition-metal complexes with open-shell singlet 1D metallic chains exhibiting large third-order optical nonlinearity.

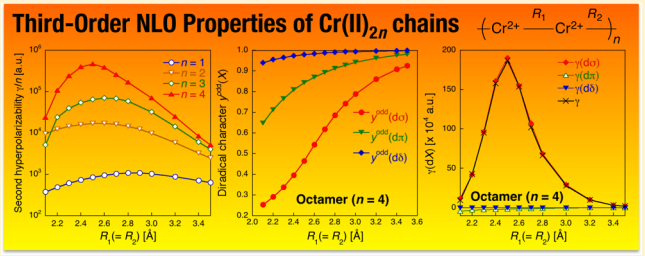

1. INTRODUCTION

Recently, open-shell singlet molecules have been theoretically proposed as a novel class of nonlinear optical (NLO) systems.[1] The key factors for enhancing the second hyperpolarizability γ (the third-order NLO property at the molecular scale) in singlet diradical systems are the intermediate diradical character[2] and the distance between the diradical electrons.[1b,3] The former represents the sensitivity of the diradical electrons to the applied electric field, while the latter corresponds to the distance of the field-induced charge transfer. These two factors, however, are generally antagonistic, because a large distance between diradical electrons leads to a large diradical character, whereas an intermediate diradical character often requires a relatively small diradical distance to achieve an intermediate overlap between the α and β spatial orbitals. One way to attenuate this trade-off relationship consists of building open-shell singlet one-dimensional (1D) systems, referred to as "1D multiradicalization",[3c] with tuned multiple diradical characters. Indeed, if the radical sites are aligned with an appropriate distance as shown in Scheme 1, the distance between both-end radicals can be elongated while keeping intermediate interactions between these radicals, which should give rise to a nonlinear enhancement of γ as a function of increasing chain length (number of radical sites). Such an increase in γ of open-shell singlet multiradical chains was computationally substantiated using model hydrogen chains (H_n).[4]

Scheme 1. One-Dimensional Open-Shell Singlet Systems with an Intermediate Open-Shell (Multiradical) Character[a]

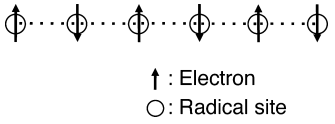

[a]The electron arrows indicate the up and down spins.

On the other hand, 1D transition-metal-atom chain complexes such as extended metal atom chains (EMACs) have attracted a great deal of attention due to their interesting bond nature and physicochemical properties, including electronic and magnetic properties.[5−12] They are also of interest from the viewpoint of the open-shell singlet because some 1D transition-metal-atom chains with even-numbered cores can present 1D multiradical characters originating from d−d orbital interactions.[5] For example, 1D tetrachromium(II) and tetramolybdenum(II) systems (Cr^{II}_4 and Mo^{II}_4) have been

Received: June 7, 2014
Published: July 24, 2014

   dx.doi.org/10.1021/ic501334p | Inorg. Chem. 2014, 53, 8700−8707

predicted to present 1D tetraradical characters of dσ, dπ, and dδ orbitals, which are controllable through the metal−metal bond length.[13] The 1D multiradical nature of singlet transition-metal-atom chains is expected to strongly enhance their third-order NLO properties. In a previous study,[3c] using the spin-unrestricted coupled cluster singles and doubles with perturbative triples UCCSD(T) method, we revealed that 1D Cr^{II}_4 and Mo^{II}_4 are σ-dominant third-order NLO systems,[3a,b] whose γ values are enhanced by dσ electrons with an intermediate open-shell character (tetraradical character), and that their γ values are significantly enhanced in comparison to those of their dimetallic analogues, which supports our speculation on the third-order NLO properties of open-shell singlet 1D transition-metal-atom chain complexes. In the present study, we investigate the γ values of open-shell singlet 1D chromium(II) chains Cr^{II}_{2n} (n = 1−4) with equivalent Cr^{II}−Cr^{II} bond lengths in relation to their open-shell characters. To confirm our hypothesis, the chain length dependence of γ is revealed by comparing chromium(II) chains with different n values. In addition to regular chains, we address chromium(II) chains with alternating R_1 and R_2 bond lengths, defining a bond-length alternation (BLA) (see Figure 1). Indeed, in real transition-metal-atom chain complexes, the metal−metal bonds have different lengths, depending on their ligands, while there are many bonding patterns and the number of them increases with chain length.[5−12] On the basis of these results, we propose guiding principles for designing highly efficient third-order NLO compounds with open-shell singlet 1D transition-metal-atom chains.

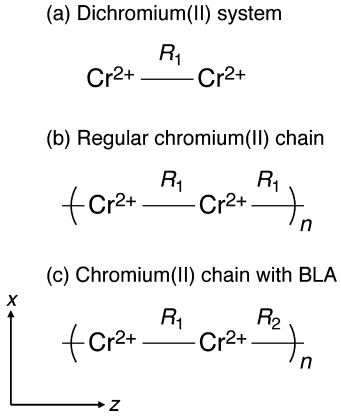

Figure 1. Structures of model systems: (a) dichromium(II) system; (b) chromium(II) chain Cr^{II}_{2n} (n = 2−4) without bond-length alternation (BLA; referred to as regular Cr^{II}_{2n}); (c) BLA Cr^{II}_{2n} (n = 2−4). R_1 and R_2 represent the bond lengths.

2. THEORETICAL AND COMPUTATIONAL ASPECTS

2.1. Model Systems. Figure 1 shows the model systems examined in this study: dichromium(II) (Cr^{II}_2) (a), 1D regular chromium(II) chains with equivalent bond lengths (regular Cr^{II}_{2n}, n = 2−4) (b), and 1D chromium(II) chains with bond-length alternation (bond lengths R_1 and R_2) (BLA Cr^{II}_{2n}, n = 2−4) (c). The d_{z^2}−d_{z^2}, d_{yz}−d_{yz}, d_{xz}−d_{xz}, d_{xy}−d_{xy}, and $d_{x^2-y^2}$−$d_{x^2-y^2}$ orbital interactions in Cr^{II}_{2n} lead to 2n dσ, dπ, dπ′, dδ, and dδ′ orbitals, respectively (5 × 2n orbitals in total). The dπ′ orbitals are rotated by 90° with respect to the dπ orbitals around the bond axis (defined as the z axis), while the dδ and dδ′ orbital sets are rotated 45° with respect to each other. The 4 × 2n d electrons formally occupy the lowest n orbitals of each dσ, dπ, dπ′, and dδ symmetry, though in the UHF formalism the highest n natural orbitals (NOs) of each symmetry possess fractional occupation numbers smaller than 1. This electron configuration leads to the 2n radical nature for each dσ, dπ, dπ′, and dδ orbital in Cr^{II}_{2n}, resulting in a quadruple 2n radical nature for the whole system. As an example, Figure 2 shows the dσ-, dπ-, dπ′-, and dδ-type NOs with their occupation numbers for regular Cr^{II}_4 with R_1 = 2.5 Å obtained by the UHF method. For each orbital symmetry, the highest two NOs (LUNO and LUNO+1) possess relatively large occupation numbers, the feature of which leads to the emergence of the tetraradical character in dσ, dπ, dπ′, and dδ orbitals and thus a quadruple tetraradical nature in Cr^{II}_4. In order to clarify the bond length dependence of the 2n radical character (open-shell character) and thus to quest for optimal bond lengths to maximize γ, the bond length R_1 is varied from 2.1 to 3.5 Å, the range of which includes the typical experimental bond lengths 2.0−2.6 Å.[5]

The UHF spin density distributions of regular Cr^{II}_{2n} (n = 2−4) with R_1 = 2.5 Å are shown in Figure 3 for each type of occupied d MO. Note that the spin polarization, which results from the broken-symmetry solution, is an artifact but it helps to analyze the spatial spin correlation.[14,15] For all systems, the α and β spin densities display an alternating pattern in accordance with Scheme 1, demonstrating that these systems meet our strategy of 1D multiradicalization. For dπ electron contributions, since the dπ and dπ′ orbitals present the same open-shell character and the same contributions to γ, we discuss only the contribution of one set (dπ orbitals).

2.2. Calculation of Open-Shell Character. The singlet multiradical nature is quantitatively characterized by the open-shell character evaluated from quantum chemical calculations. Here, the open-shell character of the dX orbitals (y^{odd}(dX), where X = σ, π, δ) is

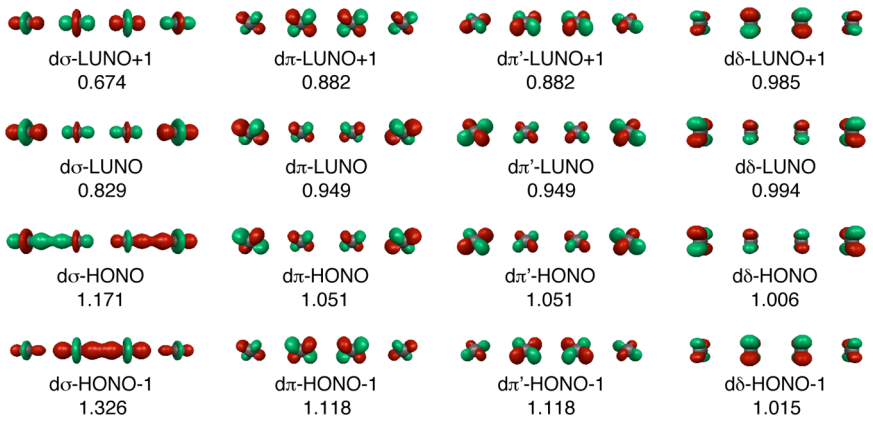

Figure 2. dσ, dπ, dπ′, and dδ natural orbitals (NOs) and their occupation numbers for regular Cr^{II}_4 with R_1 = 2.5 Å calculated using the UHF method. The red and green surfaces represent positive and negative NOs with contour values of ±0.10 a.u., respectively.

dx.doi.org/10.1021/ic501334p | Inorg. Chem. 2014, 53, 8700−8707

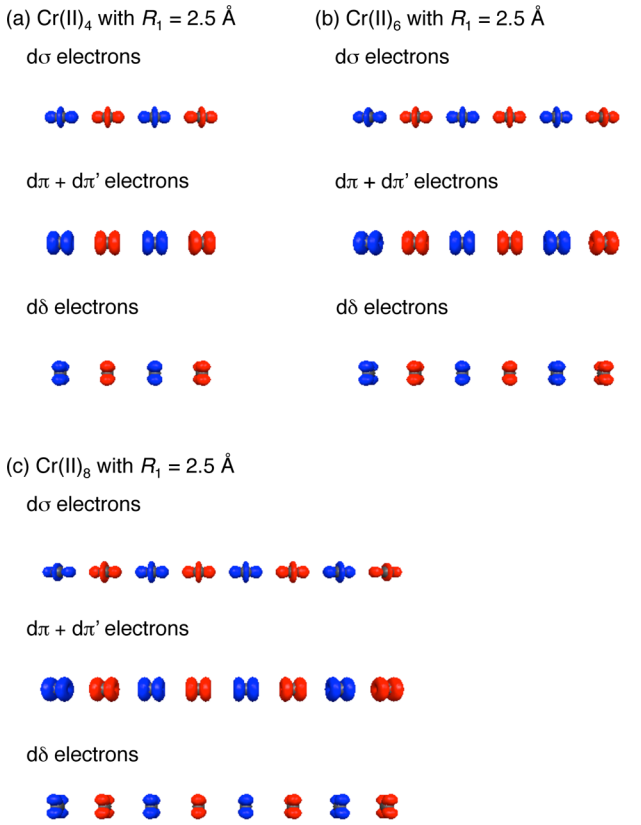

Figure 3. Spin density distributions of dσ, (dπ + dπ′), and dδ electrons for regular Cr^{II}_4 (a), Cr^{II}_6 (b), and Cr^{II}_8 (c) with a bond length (R_1) of 2.5 Å obtained from UHF molecular orbitals. The red and blue surfaces represent α and β spin densities with contour values of ±0.05 a.u., respectively.

defined as the total odd electron number ($N^{odd}(dX)$) of the 2n dX NOs divided by the maximum odd electron number (N^{odd}_{max}) (2n in the present case):[2c,3]

$$y^{odd}(dX) = \frac{\sum_{k=1}^{2n} n_k^{odd}(dX)}{N_{max}^{odd}} = \frac{N^{odd}(dX)}{N_{max}^{odd}} \quad (1)$$

where the odd electron number is obtained according to Head-Gordon:[16]

$$n_k^{odd}(dX) \equiv \min\{2 - n_k(dX), n_k(dX)\} \quad (2)$$

$n_k(dX)$ is the occupation number of the kth dX NO. $y^{odd}(dX)$ values range from 0 to 1, which correspond to the closed-shell and pure open-shell states, respectively. In the present study, we employ the UHF method combined with a spin-projection correction[2b,c,17] (referred to as the PUHF method) to obtain the open-shell characters because the PUHF method reproduces the open-shell characters of Cr^{II}_2 and Cr^{II}_4 calculated with the highly electron-correlated method: i.e., spin-unrestricted coupled-cluster singles and doubles (UCCSD) (see the Supporting Information).

2.3. Evaluation and Analysis of Static Second Hyperpolarizability. The longitudinal γ_{zzzz} (≡γ) tensor components (with z the bond axis) were calculated using the finite-field (FF) approach.[18] This time, γ is obtained as the first-order differentiation of the first hyperpolarizability (β) with respect to the applied external electric field, which allows minimizing the numerical error. The β values are calculated using the coupled perturbed Kohn–Sham (CPKS) method.[19] The perturbation series expansion convention (called the B convention[20]) is chosen for defining γ and the following first-order numerical differentiation formula is employed:

$$\gamma = \frac{1}{3} \times \frac{\beta(3F) - 9\beta(2F) + 45\beta(F) - 45\beta(-F) + 9\beta(-2F) - \beta(-3F)}{60F} \quad (3)$$

Here, $\beta(F)$ is the first hyperpolarizability (B convention) in the presence of the static electric field F in the z direction. It is noted that the Gaussian 09 program package[21] employs the T convention (Taylor series expansion) to calculate β, so that the obtained β values are converted from the T to B convention using the relation $2\beta^B = \beta^T$.[20] We used F values ranging from 0.0002 to 0.0015 a.u. to obtain numerically stable γ values. The γ values are given in a.u.: 1.0 a.u. of γ is equal to 6.235377×10^{-65} C^4 m^4 J^{-3} and 5.0367×10^{-40} esu. For the calculation of γ, we employed the long-range corrected UBLYP (LC-UBLYP) method with a range-separating parameter (μ) of 0.8 $bohr^{-1}$ (referred to as LC-UBLYP(0.8)), which was demonstrated to be reliable to calculate γ in dimetallic systems with a transition-metal–transition-metal bond.[22] Note that this optimal μ value for metal–metal-bonded systems is larger than that (μ = 0.33 $bohr^{-1}$) for small-size organic π-conjugated systems.[23] This difference in the optimal μ values is understood by the fact that μ^{-1} represents an effective electron screening (delocalization) length or the characteristic radius of a molecule.[24] The fact that the optimal μ value of metal–metal dσ bonded systems is larger than that of pπ delocalized organic systems means that dσ bonds are more localized than pπ bonds. It is also noted that to include relativistic effects, we used the SDD basis sets,[25] the effective core potential (ECP) of which has been shown to well reproduce the Dirac–Hartree–Fock γ values obtained with an all-electron basis set.[26] We should also pay attention to the diffuse basis

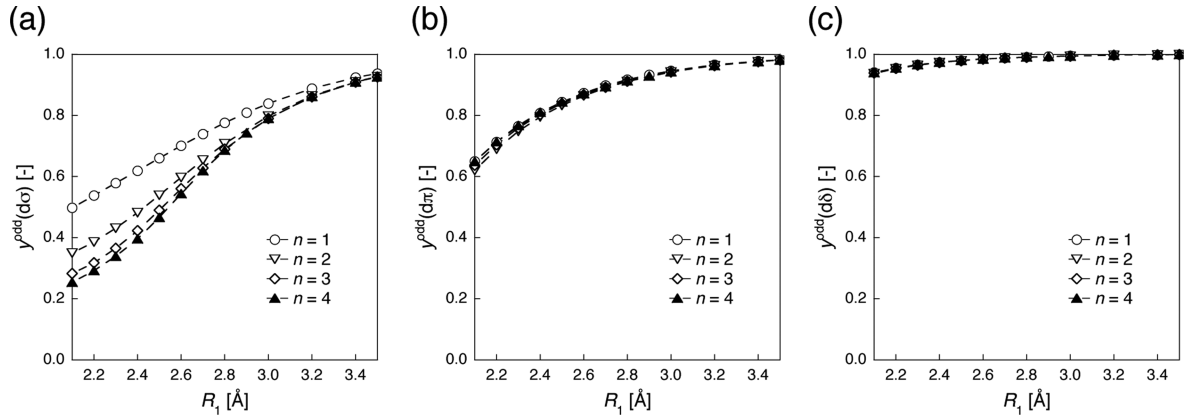

Figure 4. Bond length (R_1) dependences of the open-shell characters $y^{odd}(d\sigma)$ (a), $y^{odd}(d\pi)$ (b), and $y^{odd}(d\delta)$ (c) for regular Cr^{II}_{2n} (n = 1–4) calculated using the PUHF/SDD method.

dx.doi.org/10.1021/ic501334p | Inorg. Chem. 2014, 53, 8700–8707

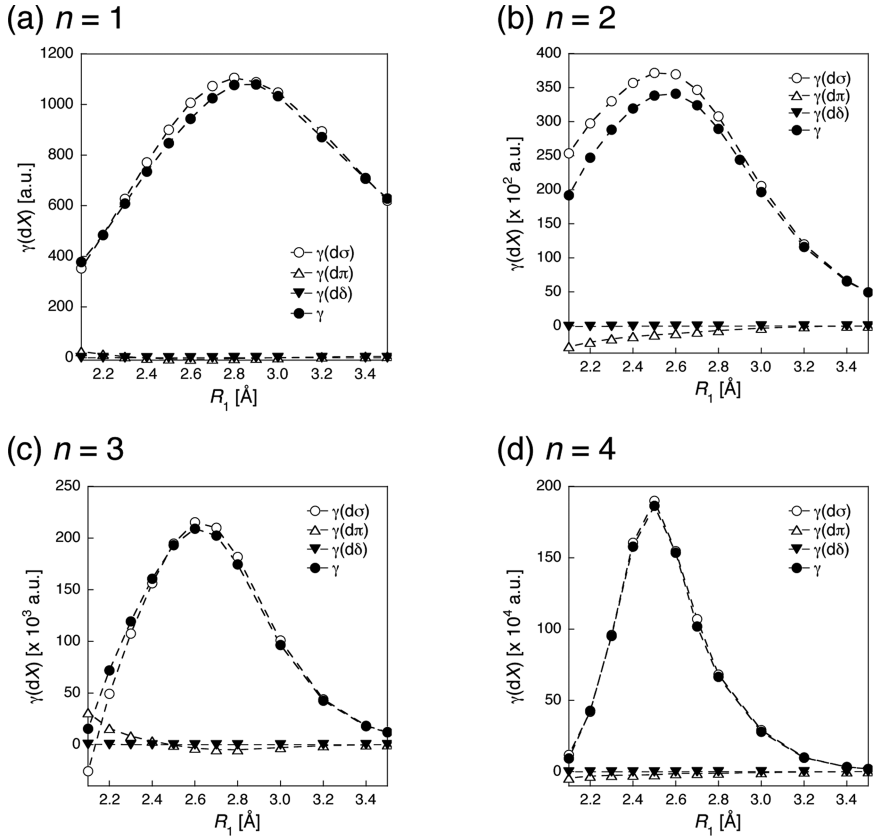

Figure 5. Bond length (R_1) dependences of γ and of its dX orbitals contributions in regular chains Cr^{II}_2 (n = 1) (a), Cr^{II}_4 (n = 2) (b), Cr^{II}_6 (n = 3) (c), and Cr^{II}_8 (n = 4) (d), calculated using the LC-UBLYP(0.8)/SDD method.

functions because, as for closed-shell systems,[27] extended basis sets (with diffuse functions) might be indispensable for obtaining quantitative γ values in open-shell singlet systems.[28] The SDD basis set is expected to be sufficiently extended, since it already includes one set of diffuse s, two sets of diffuse p, and one set of diffuse d functions. Indeed, the addition of a set of d and f diffuse functions to the SDD basis set only provides small variations of the γ value of Cr^{II}_2 at the UCCSD and UCCSD(T) levels of approximation (see the Supporting Information of ref 3a).

For a detailed analysis of γ, the contributions of the dX electrons (γ(dX), where X = σ, π, δ) are calculated using a partitioning scheme[2c,3] and the expression

$$\gamma(\mathrm{dX}) = -\frac{1}{3!}\int r_z \rho^{(3)}_{zzz}(\mathrm{dX})\,\mathrm{d}r \tag{4}$$

where $\rho^{(3)}_{zzz}$(dX) is referred to as the γ(dX) density[29] and is determined by the third-order derivative of the electron density of the set of dX NOs with respect to the electric field in the z direction, and it reads

$$\rho^{(3)}_{zzz}(\mathrm{dX}) = \frac{\partial^3}{\partial F_z^3}\left\{\sum_{k=1}^{2n} n_k(\mathrm{dX})|\phi_k^{\mathrm{dX}}(r)|^2\right\}\Bigg|_{F_z=0} \tag{5}$$

Here, $\phi_k^{\mathrm{dX}}(r)$ is the kth NO of dX symmetry. The positive and negative γ(dX) densities multiplied by F_z^3 represent respectively the field-induced increase and decrease in the dX electron density in proportion to F_z^3, which are at the origin of the third-order dipole moment in the direction from positive to negative γ(dX) densities. The γ(dX) value and its density are calculated by the LC-UBLYP(0.8)/SDD method. Note that the γ values obtained from the numerical first-order derivative of analytical β match closely those obtained from the γ densities (eq 4) within an error of 5%.

All calculations on y^{odd}(dX) and γ were performed with the Gaussian 09 program package.

3. RESULTS AND DISCUSSION

3.1. Size Dependence of Open-Shell Character in Regular Chromium(II) Chains. Figure 4 shows the bond length (R_1) dependences of y^{odd}(dσ), y^{odd}(dπ), and y^{odd}(dδ) for regular Cr^{II}_{2n} (n = 1−4), calculated at the PUHF/SDD level. In all systems, the open-shell characters monotonically increase as a function of the bond length. This tendency originates from the weakness in the d−d orbital interactions, which leads to the emergence of multiradical nature. All systems present the following order of the open-shell characters within the R_1 region, y^{odd}(dδ) > y^{odd}(dπ) > y^{odd}(dσ), which is also rationalized by the relative d−d orbital interactions: decreasing from d_{xy} (forming the dδ MOs) through d_{xz} and d_{yz} (dπ MOs) to d_{z^2} (dσ MOs). Regular Cr^{II} chains with different n values show almost the same bond length dependences of y^{odd}(dπ) and y^{odd}(dδ) (see Figure 4b,c), indicating that a given bond length leads to the same multiradical natures of dπ and dδ orbitals regardless of chain length. In contrast, the dσ orbitals show a significant chain length dependence of the open-shell character when R_1 < ∼3.0 Å (Figure 4a). y^{odd}(dσ) decreases as a function of n, though the difference between n = 3 and n = 4 becomes small, predicting that dσ open-shell character converges around n = 4 with increasing chain length. Such a difference in the chain length dependences of y^{odd}(dX), which are related to the effective bond order, indicates that the delocalization effects are mostly associated with the dσ electrons.

3.2. Metal−Metal Bond Length Dependences of γ in Regular Chromium(II) Chains with Different Chain Lengths. Figure 5 displays the variations in γ and γ(dX) as a

dx.doi.org/10.1021/ic501334p | Inorg. Chem. 2014, 53, 8700−8707

function of the bond length R_1 in regular Cr^{II}_{2n} (n = 1−4) as calculated using the LC-UBLYP(0.8)/SDD method. Bell-shaped behaviors of γ are observed for all systems, though the maximum γ (γ_{max}) value and the bond length giving γ_{max} (R_{1max}) depend on n. The Cr^{II}_8 (n = 4) compound shows a rapid variation in γ around R_{1max} in comparison to other systems, which predicts that the fine control of the bond lengths is crucial for realizing large third-order NLO properties in large/long 1D transition-metal chains. Similar to a previous study, which clarifies the dominant dσ contribution in tetrametallic transition-metal systems,[3c] the contribution of dσ electrons (γ(dσ)) is dominant in regular Cr^{II}_6 and Cr^{II}_8 as in Cr^{II}_2 and Cr^{II}_4, while those of dπ and dδ electrons are negligible (see Figure 5), which allows us to focus on the dσ contribution in the analysis of γ. The bond lengths and dσ open-shell characters (y^{odd}_{max}(dσ)) corresponding to γ_{max}(dσ) for regular Cr^{II}_{2n} (n = 1−4) are given with their γ_{max}(dσ) values in Table 1.

Table 1. Bond Lengths (R_1) and dσ Open-Shell Characters (y^{odd}_{max}(dσ)) Corresponding to γ_{max}(dσ) for Regular Cr^{II}_{2n} (n = 1−4) together with Their γ_{max}(dσ) Values

n	R_1 (Å)	y^{odd}_{max}(dσ)[a]	γ_{max}(dσ)[b] (a.u.)
1	2.8	0.776	111 × 10
2	2.5	0.539	372 × 10^2
3	2.6	0.560	215 × 10^3
4	2.5	0.466	190 × 10^4

[a]Obtained using the PUHF/SDD method. [b]Calculated at the LC-UBLYP(0.8)/SDD level of theory.

The y^{odd}_{max}(dσ) values of regular Cr^{II}_{2n} for n = 1−4 amount to 0.466−0.776, demonstrating that the γ(dσ) enhancement is associated with intermediate dσ open-shell character. Then, y^{odd}_{max}(dσ) decreases as a function of chain length except for the slight inversion between n = 2, 3. A similar tendency was observed in an open-shell singlet 1D hydrogen atom chain (H_{2n}): the PUHF average diradical character (equivalent to the PUHF open-shell character in this study) corresponding to γ_{max} decreases as a function of H_{2n} chain length.[4] On the basis of the results on open-shell singlet 1D Cr^{II}_{2n} and H_{2n}, the decrease in y^{odd}_{max} as a function of chain length is predicted to be a general property of open-shell singlet 1D multiradical systems. The fact that extending the chain length leads to an increase in electron delocalization and an enhancement of the γ amplitude may be related to the decrease of open-shell character maximizing γ. Figure 6 compares the bond length (R_1) dependences of γ per n for regular Cr^{II}_{2n} chains with n = 1−4. Increasing chain length is found to extraordinarily enhance the γ_{max}/n value: 1080 a.u. (n = 1), 170 × 10^2 a.u. (n = 2), 697 × 10^2 a.u. (n = 3), and 466 × 10^3 a.u. (n = 4). On the other hand, the bond length giving γ_{max} (R_{1max}) decreases with n from n = 1 (R_{1max} = 2.9 Å) to n = 2, 3 (2.6 Å) and n = 4 (2.5 Å), predicting a further decrease in R_{1max} for regular Cr^{II}_{2n} chains with larger n values.

The dominant γ(dσ) contribution was then analyzed by using the γ(dσ) density distribution calculated by eq 5. Figure 7 displays the γ(dσ) density distributions of regular Cr^{II}_{2n} with R_{1max} at the LC-UBLYP(0.8)/SDD level of theory. It is found that the positive and negative γ(dσ) densities of Cr^{II}_2 are distributed on the terminal atoms and that their distributions are well separated (see Figure 7a). In regular Cr^{II}_{2n} with n = 2−4, the positive and negative γ(dσ) densities are also distributed on the terminal atoms—leading to a positive γ(dσ) value—while positive and negative γ(dσ) densities alternate in the

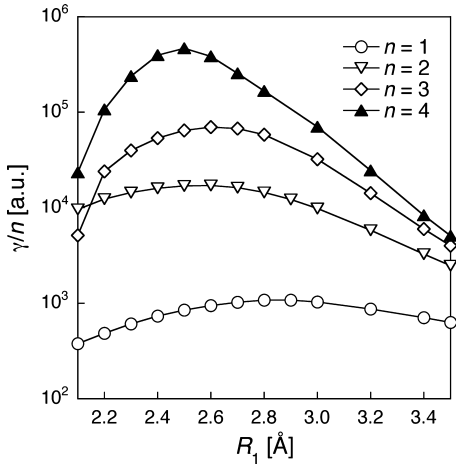

Figure 6. Variations in γ per n (γ/n) of regular Cr^{II}_{2n} chains (n = 1−4) as a function of the metal−metal bond length (R_1) calculated using the LC-UBLYP(0.8)/SDD method.

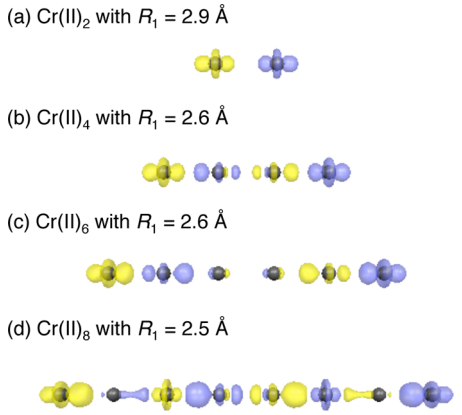

Figure 7. γ(dσ) density distributions for Cr^{II}_2 with R_{1max} (2.9 Å) (a), regular Cr^{II}_4 with R_{1max} (2.6 Å) (b), regular Cr^{II}_6 with R_{1max} (2.6 Å) (c), and regular Cr^{II}_8 with R_{1max} (2.5 Å) (d) calculated at the LC-UBLYP(0.8)/SDD level of theory. The yellow and blue surfaces represent positive and negative densities with contour values of ±30, ±500, ±2000, and ±7500 a.u. for Cr^{II}_2, Cr^{II}_4, Cr^{II}_6, and Cr^{II}_8, respectively.

internal regions and mostly cancel each other. As a result, the positive and negative γ(dσ) densities on the both-end atoms provide the largest contribution to γ(dσ), because they display the largest intervals (see eq 4). Therefore, the γ(dσ) density distributions indicate that the dσ radical electrons on the both-end atoms give dominant contributions to γ(dσ) in regular Cr^{II} chains with an intermediate dσ open-shell character. This feature exemplifies the enhancement mechanism of γ by the 1D multiradicalization.

3.3. BLA Effects on γ. To reveal BLA effects on γ, we introduce the BLA to Cr^{II} chains in two ways: (A) changing R_2 while keeping R_1 constant (=R_{1max} of regular Cr^{II} chains; i.e., 2.6 Å for Cr^{II}_4 and Cr^{II}_6 and 2.5 Å for Cr^{II}_8) and (B) changing R_1 while keeping R_2 constant in the same way as for (A) (see Figure 2c). The BLA is characterized by the R_2/R_1 ratio, where R_2/R_1 = 1.00 corresponds to regular Cr^{II} chains with γ_{max} and R_{1max}. The γ enhancement ratio with respect to regular chains reads

dx.doi.org/10.1021/ic501334p | Inorg. Chem. 2014, 53, 8700−8707

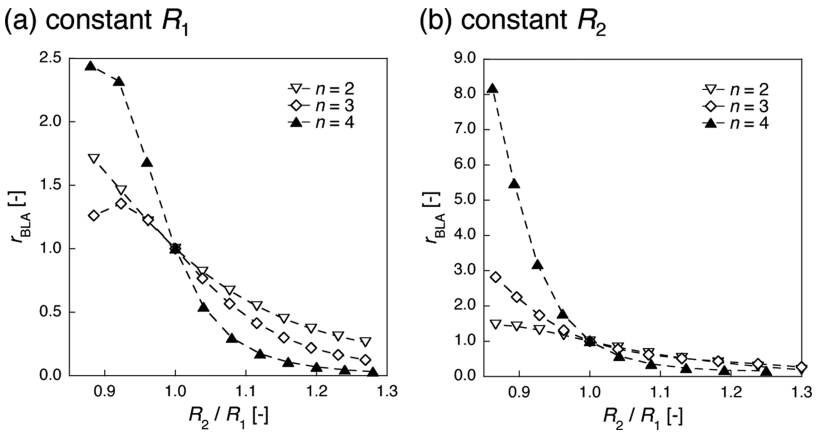

Figure 8. Variations in r_{BLA} as a function of R_2/R_1 for BLA Cr^{II}_{2n} (n = 2−4) with constant R_1 (a) or R_2 (b). The constant bond length is set to the R_{1max} value of the regular Cr^{II} chains: i.e., 2.6 Å for Cr^{II}_4 and Cr^{II}_6 and 2.5 Å for Cr^{II}_8.

$$r_{BLA} = \frac{\gamma(\text{BLA})}{\gamma_{max}(\text{regular})} \quad (6)$$

r_{BLA} > 1 and r_{BLA} < 1 correspond therefore to BLA-induced increase or decrease in γ. Figure 8 shows the variations in r_{BLA} as a function of R_2/R_1 for Cr^{II}_{2n} with n = 2−4. For all BLA chains with constant R_1 (Figure 8a), on going from R_2/R_1 = 0.9 to 1.3, r_{BLA} decreases as a function of R_2/R_1. Thus, when R_2 > R_1, γ decreases as a function of the BLA, while for R_2 < R_1 the opposite is observed. The BLA chains with constant R_2 display behavior similar to those with constant R_1 (see parts a and b of Figure 8), though the γ enhancement ratio for n = 4 with R_2/R_1 < 1 is larger than that for the n = 4 chain with constant R_1. The largest enhancement of γ is observed for BLA Cr^{II}_8 (n = 4) with constant R_2 (r_{BLA} = 8.18 at R_2/R_1 = 0.862), showing further enhancement of γ in longer alternating chains. Note that both the γ enhancement when R_2 < R_1 and the γ reduction when R_2 > R_1 were already observed in an open-shell singlet 1D H_4 chain.[30] This similar tendency demonstrates that these BLA effects are general features of open-shell singlet 1D atomic chains and also that H_2 chains are reliable model systems. Then, the significant BLA dependence of γ indicates the wide-range controllability of γ in open-shell singlet 1D transition-metal chains by adjusting the metal−metal bond lengths and BLA through the ligand modifications.

4. CONCLUSIONS

We have investigated the bond length dependence of γ in open-shell singlet 1D Cr^{II}_{2n} chains (n = 1−4) with equivalent Cr−Cr bond lengths (R_1) referred to as "regular Cr^{II}_{2n}" using the LC-UBLYP method with a range separating parameter of 0.8 $bohr^{-1}$. γ values of these systems display a bell-shaped behavior as a function of R_1. The maximum γ (γ_{max}) significantly increases as a function of chain length, while the bond length (R_{1max}) giving γ_{max} decreases. This result indicates the possibility of further enhancement of γ_{max} in large regular Cr^{II} chains with smaller R_{1max}. The partitioning scheme of γ has revealed that the dσ electrons dominantly contribute to γ, while the dπ and dδ electrons provide negligible contributions, which indicates that the regular Cr^{II} chains belong to a novel class of "σ-dominant" third-order NLO systems. The enhancement of γ in Cr^{II} chains is attributed to the large amplitude of field-induced charge transfer of dσ electrons between the both-end atom sites through the dσ bonding interactions, which is realized by its intermediate dσ open-shell character and by the large intervals between the both-end atoms. These results predict that open-shell singlet polynuclear transition-metal complexes with metal atom chains such as extended metal atom chain (EMAC) complexes also belong to "σ-dominant" third-order NLO systems. Moreover, we have investigated the effects of bond-length alternation (BLA) on γ in open-shell singlet 1D Cr^{II} chains. We have examined the BLA Cr^{II}_{2n} (n = 2−4) with two kinds of Cr−Cr bond lengths: R_1 and R_2. It is found that the BLA with both-end bond lengths larger than the adjacent internal bond length (R_1 > R_2) enhances γ, while the BLA with an inverse R_1 and R_2 relation (R_1 < R_2) tends to decrease γ. These BLA effects on γ are further intensified by increasing the chain length. For example, the γ values of BLA Cr^{II}_4 with R_2/R_1 = 0.75 and BLA Cr^{II}_8 with R_2/R_1 = 0.9 are more than twice as large as the γ_{max} values of regular Cr^{II}_4 and Cr^{II}_8, respectively. The present results indicate the wide range controllability of γ by tuning the metal−metal bond lengths and the BLAs in open-shell singlet 1D transition-metal chain complexes, which can be achieved by ligand modifications.[31] Recent theoretical studies have clarified that dσ contributions to γ are also dominant and are maximized in the intermediate diradical character y(dσ) region not only in bare transition-metal bonded systems but also in transition-metal complexes including equatorial[32a] and axial[32b] ligands. Although we have focused on a *regular* BLA, the transition-metal-atom chain complexes could possess a variety of bonding patterns depending on the ligands[5−12] and various combinations of heterometals.[33] At the next stage, the investigations will focus on the variety of bonding patterns and on the heterometal effects on γ, which will further highlight the structural conditions for maximizing the third-order NLO properties in open-shell singlet 1D transition-metal chain complexes. In addition, to confirm the validity of the present theoretical predictions, the synthesis of EMACs with various open-shell characters and the experimental determination of their third-order NLO properties, e.g., two-photon absorption, are intensely desired.

■ ASSOCIATED CONTENT

Supporting Information

Text and figures describing the open-shell characters of Cr^{II}_2 and Cr^{II}_4 at the UHF, PUHF, and UCCSD levels of approximation. This material is available free of charge via the Internet at http://pubs.acs.org.

dx.doi.org/10.1021/ic501334p | Inorg. Chem. 2014, 53, 8700−8707

AUTHOR INFORMATION

Corresponding Author

*M.N.: fax, +81-6-6850-6268; e-mail, mnaka@cheng.es.osaka-u.ac.jp.

Notes

The authors declare no competing financial interest.

ACKNOWLEDGMENTS

This work was supported by a Grant-in-Aid for Bilateral Programs Joint Research Projects (JSPS-FRS-FNRS), a Grant-in-Aid for Scientific Research (A) (No. 25248007) from the Japan Society for the Promotion of Science (JSPS), a Grant-in-Aid for Scientific Research on Innovative Areas (No. A24109002a), MEXT, the Strategic Programs for Innovative Research (SPIRE), MEXT, the Computational Materials Science Initiative (CMSI) of Japan, the Academy Louvain (ARC "Extended π-Conjugated Molecular Tinkertoys for Optoelectronics, and Spintronics"), and the Belgian Government (IUAP program No. P06-27 "Functional Supramolecular Systems"). H.F. expresses his special thanks for a JSPS Research Fellowship for Young Scientists. Theoretical calculations were partially performed at the Research Center for Computational Science, Okazaki, Japan.

REFERENCES

(1) (a) Nakano, M.; Kishi, R.; Nitta, T.; Kubo, T.; Nakasuji, K.; Kamada, K.; Ohta, K.; Champagne, B.; Botek, E.; Yamaguchi, K. *J. Phys. Chem. A* **2005**, *109*, 885−891. (b) Nakano, M.; Kishi, R.; Ohta, S.; Takahashi, H.; Kubo, T.; Kamada, K.; Ohta, K.; Botek, E.; Champagne, B. *Phys. Rev. Lett.* **2007**, *99*, 033001−1−4. (c) Lambert, C. *Angew. Chem., Int. Ed.* **2011**, *50*, 1756−1758. (d) Sun, Z.; Wu, J. *J. Mater. Chem.* **2012**, *22*, 4151−4160.

(2) (a) Hayes, E. F.; Siu, A. K. Q. *J. Am. Chem. Soc.* **1971**, *93*, 2090−2091. (b) Yamaguchi, K. In *Self-Consistent Field: Theory and Applications*; Carbo, R.; Klobukowski, M., Eds.; Elsevier: Amsterdam, 1990; p 727−828. (c) Nakano, M.; Fukui, H.; Minami, T.; Yoneda, K.; Shigeta, Y.; Kishi, R.; Champagne, B.; Botek, E.; Kubo, T.; Ohta, K.; et al. *Theor. Chem. Acc.* **2011**, *130*, 711−724, *erratum*, 725−726.

(3) (a) Fukui, H.; Nakano, M.; Shigeta, Y.; Champagne, B. *J. Phys. Chem. Lett.* **2011**, *2*, 2063−2066. (b) Fukui, H.; Inoue, Y.; Yamada, T.; Ito, S.; Shigeta, Y.; Kishi, R.; Champagne, B.; Nakano, M. *J. Phys. Chem. A* **2012**, *116*, 5501−5509. (c) Fukui, H.; Nakano, M.; Champagne, B. *Chem. Phys. Lett.* **2012**, *527*, 11−15.

(4) Nakano, M.; Takebe, A.; Kishi, R.; Ohta, S.; Nate, M.; Kubo, T.; Kamada, K.; Ohta, K.; Champagne, B.; Botek, E.; et al. *Chem. Phys. Lett.* **2006**, *432*, 473−479.

(5) Cotton, F. A.; Murillo, C. A.; Walton, R. A. *Multiple Bonds between Metal Atoms*, 3rd ed.; Springer: New York, 2005.

(6) Parkin, G. Metal-Metal Bonding. In *Structure and Bonding (Berlin)*; Mingos, D. M. P., Ed.; Springer: Heidelberg, Germany, 2010; Vol. *136*.

(7) Michael Springborg, M.; Dolg, Y. *Metallic Chains/Chains of Metals*, 1st ed.; Elsevier: Amsterdam, 2007.

(8) Bera, J. K.; Dunbar, K. R. *Angew. Chem., Int. Ed.* **2002**, *41*, 4453−4457.

(9) Ismailov, R.; Weng, W.-Z.; Wang, R.-R.; Huang, Y.-L.; Yeh, C.-Y.; Lee, G.-H.; Peng, S.-M. *Eur. J. Inorg. Chem.* **2008**, 4290−4295.

(10) Tatsumi, Y.; Murahashi, T.; Okada, M.; Ogoshi, S.; Kurosawa, H. *Chem. Commun.* **2008**, 477−479.

(11) Mashima, K. *Bull. Chem. Soc. Jpn.* **2010**, *83*, 299−312.

(12) (a) Kuo, J.-H.; Tsao, T.-B.; Lee, G.-H.; Lee, H.-W.; Yeh, C.-Y.; Peng, S.-M. *Eur. J. Inorg. Chem.* **2011**, 2025−2028. (b) Ismayilov, R. H.; Wang, W.-Z.; Lee, G.-H.; Yeh, C.-Y.; Hua, S.-A.; Song, Y.; Rohmer, M.-M.; Bénard, M.; Peng, S.-M. *Angew. Chem., Int. Ed.* **2011**, *50*, 2045−2048.

(13) (a) Nishino, M.; Yamanaka, S.; Yoshioka, Y.; Yamaguchi, K. *J. Phys. Chem. A* **1997**, *101*, 705−712. (b) Nishino, M.; Yoshioka, Y.; Yamaguchi, K.; Mashima, K.; Tani, K.; Nakamura, A. *Bull. Chem. Soc. Jpn.* **1998**, *71*, 99−112.

(14) Yoneda, K.; Nakano, M.; Inoue, Y.; Inui, T.; Fukuda, K.; Shigeta, Y.; Kubo, T.; Champagne, B. *J. Phys. Chem. C* **2012**, *116*, 17787−17795.

(15) Mizukami, W.; Kurashige, Y.; Yanai, T. *J. Chem. Theory. Comput.* **2013**, *9*, 401−407.

(16) Head-Gordon, M. *Chem. Phys. Lett.* **2003**, *372*, 508−511.

(17) Yamanaka, S.; Okumura, M.; Nakano, M.; Yamaguchi, K. *J. Mol. Struct. (THEOCHEM)* **1994**, *310*, 205−209.

(18) Cohen, H. D.; Roothaan, C. C. J. *J. Chem. Phys.* **1965**, *43*, S34−S39.

(19) (a) Colwell, S. M.; Murray, C. W.; Handy, N. C.; Amos, R. D. *Chem. Phys. Lett.* **1993**, *210*, 261−268. (b) Lee, A. M.; Colwell, S. M. *J. Chem. Phys.* **1994**, *101*, 9704−9709.

(20) Willetts, A.; Rice, J. E.; Burland, D. M.; Shelton, D. P. *J. Chem. Phys.* **1992**, *97*, 7590−7599.

(21) Frisch, M. J.; Trucks, G. W.; Schlegel, H. B.; Scuseria, G. E.; Robb, M. A.; Cheeseman, J. R.; Scalmani, G.; Barone, V.; Mennucci, B.; Petersson, G. A.; Nakatsuji, H.; Caricato, M.; Li, X.; Hratchian, H. P.; Izmaylov, A. F.; Bloino, J.; Zheng, G.; Sonnenberg, J. L.; Hada, M.; Ehara, M.; Toyota, K.; Fukuda, R.; Hasegawa, J.; Ishida, M.; Nakajima, T.; Honda, Y.; Kitao, O.; Nakai, H.; Vreven, T.; Montgomery, J. A., Jr.; Peralta, J. E.; Ogliaro, F.; Bearpark, M.; Heyd, J. J.; Brothers, E.; Kudin, K. N.; Staroverov, V. N.; Kobayashi, R.; Normand, J.; Raghavachari, K.; Rendell, A.; Burant, J. C.; Iyengar, S. S.; Tomasi, J.; Cossi, M.; Rega, N.; Millam, J. M.; Klene, M.; Knox, J. E.; Cross, J. B.; Bakken, V.; Adamo, C.; Jaramillo, J.; Gomperts, R.; Stratmann, R. E.; Yazyev, O.; Austin, A. J.; Cammi, R.; Pomelli, C.; Ochterski, J. W.; Martin, R. L.; Morokuma, K.; Zakrzewski, V. G.; Voth, G. A.; Salvador, P.; Dannenberg, J. J.; Dapprich, S.; Daniels, A. D.; Farkas, Ö.; Foresman, J. B.; Ortiz, J. V.; Cioslowski, J.; Fox, D. J. *Gaussian 09, Revision A.1*; Gaussian, Inc., Wallingford, CT, 2009.

(22) Fukui, H.; Inoue, Y.; Kishi, R.; Shigeta, Y.; Champagne, B.; Nakano, M. *Chem. Phys. Lett.* **2012**, *523*, 60−64.

(23) (a) Kamiya, M.; Sekino, J.; Tsuneda, T.; Hirao, K. *J. Chem. Phys.* **2005**, *122*, 234111−1−10. (b) Kishi, R.; Bonness, S.; Yoneda, K.; Nakano, M.; Botek, E.; Champagne, B.; Kubo, T.; Kamada, K.; Ohta, K.; Tsuneda, T. *J. Chem. Phys.* **2010**, *132*, 094107−1−11. (c) Bonness, S.; Fukui, H.; Yoneda, K.; Kishi, R.; Champagne, B.; Botek, E.; Nakano, M. *Chem. Phys. Lett.* **2010**, *493*, 195−199.

(24) Refaely-Abramson, S.; Baer, R.; Kronik, L. *Phys. Rev. B* **2011**, *84*, 075144−1−8.

(25) Dolg, M.; Wedig, U.; Stoll, H.; Preuss, H. *J. Chem. Phys.* **1987**, *86*, 866−872.

(26) Norman, P.; Schimmelpfennig, B.; Ruud, K.; Jensen, H. J. A.; Ågren, H. *J. Chem. Phys.* **2002**, *116*, 6914−6923.

(27) (a) Hurst, G. J. B.; Dupuis, M.; Clementi, E. *J. Chem. Phys.* **1988**, *89*, 385−395. (b) Maroulis, G. *J. Chem. Phys.* **1999**, *111*, 583. (c) Maroulis, G.; Xenides, D.; Hohm, U.; Loose, A. *J. Chem. Phys.* **2001**, *115*, 7957−7967.

(28) (a) Champagne, B.; Botek, E.; Nakano, M.; Nitta, T.; Yamaguchi, K. *J. Chem. Phys.* **2005**, *122*, 114315−1−12. (b) Kishi, R.; Nakano, M.; Ohta, S.; Takebe, A.; Nate, M.; Takahashi, H.; Kubo, T.; Kamada, K.; Ohta, K.; Botek, E.; et al. *J. Chem. Theory Comput.* **2007**, *3*, 1699−1707.

(29) Nakano, M.; Shigemoto, I.; Yamada, S.; Yamaguchi, K. *J. Chem. Phys.* **1995**, *103*, 4175−4191.

(30) Nakano, M.; Minami, T.; Fukui, H.; Kishi, R.; Shigeta, Y.; Champagne, B. *J. Chem. Phys.* **2012**, *136*, 0243151−1−7.

(31) (a) Nippe, M.; Turov, Y.; Berry, J. F. *Inorg. Chem.* **2011**, *50*, 10592−10599. (b) Uemura, K.; Ebihara, M. *Inorg. Chem.* **2011**, *50*, 7919−7921.

(32) (a) Inoue, Y.; Yamada, T.; Champagne, B.; Nakano, M. *Chem. Phys. Lett.* **2013**, *570*, 75−79. (b) Yamada, T.; Takamuku, S.; Matsui, H.; Champagne, B.; Nakano, M. *Chem. Phys. Lett.* **2014**, *608*, 68−73.

(33) Yamada, T.; Inoue, Y.; Champagne, B.; Nakano, M. *Chem. Phys. Lett.* **2013**, *579*, 73−77.